

Limit behavior of the magnetic coupling coefficient for mid-range, near-field applications

This content has been downloaded from IOPscience. Please scroll down to see the full text.

2013 J. Phys.: Conf. Ser. 476 012116

(<http://iopscience.iop.org/1742-6596/476/1/012116>)

View [the table of contents for this issue](#), or go to the [journal homepage](#) for more

Download details:

IP Address: 208.91.55.173

This content was downloaded on 30/06/2014 at 14:20

Please note that [terms and conditions apply](#).

Limit behavior of the magnetic coupling coefficient for mid-range, near-field applications

Emily Guthrie, Anton Frolenkov and Jose Oscar Mur-Miranda

Olin College of Engineering, Needham, MA, USA

E-mail: emily.guthrie@students.olin.edu

Abstract. We have derived compact algebraic bounds for the limit behavior of the magnetic coupling coefficient, κ , for axially aligned multilayer coils. These bounds are validated experimentally. We have also found an expression based on the coil geometry that captures its long-range magnetic behavior. In particular, the limit behavior of the magnetic coupling coefficient is the same for any pair of axially aligned multilayer coils when the separation distance is normalized by this expression.

1. Introduction

The magnetic coupling coefficient κ is a key parameter that characterizes the performance of inductive systems. Since the efficiency of inductive power transfer is proportional to the magnetic coupling coefficient squared for large enough separation distances [1, 2], these expressions bound the performance of these systems in this range. This also suggests optimal geometric coil designs that maximize the limit behavior of the magnetic coupling coefficient.

Since the mutual inductance between two filament loops is a transcendental expression that requires elliptic integrals [3], there are no general closed-form expressions for the self and mutual inductance of coils. Furthermore, even though several approximations for both self and mutual inductances of various geometries have been found [4, 5, 8], the magnetic coupling coefficient is still calculated empirically [2], derived [6], or approximated within a specific context [7, 9]. We present a simple expression that serves as a widely applicable upper bound on the magnetic coupling coefficient for a broad class of inductive systems. Furthermore, they provide a limit test for similar design equations in other configurations, such as unaligned coils, or coils with other cross sectional geometries.

2. Derivation

Figure 1 shows the specific case under consideration, consisting of axially aligned, multi-layer coils $i = 1, 2$ with separation s and characterized by their inductance L_i , turns density ρ_{Ni} , outer radius r_i , length ℓ_i , and fill factor f_i , where $0 < f_i < 1$. In the limit as the separation between sender and receiver increases, the magnetic coupling coefficient starts to decrease inversely proportional to the distance cubed, which determines the performance of mid-range inductive systems [1, 2, 10]. At this long range, while in the near field, the magnetic coupling coefficient



can be calculated by combining the mutual inductance, given by

$$L_M = \frac{\mu_0 \rho_{N1} \rho_{N2} \pi}{2} \int_0^{\ell_2} \int_{r_2(1-f_2)}^{r_2} r_2'^2 \int_0^{\ell_1} \int_{r_1(1-f_1)}^{r_1} \frac{r_1'^2}{[r_1'^2 + (s + \ell_1' + \ell_2')^2]^{3/2}} dr_1' d\ell_1' dr_2' d\ell_2',$$

with Wheeler's approximation for the self inductance [5],

$$L_i = \frac{\mu_0 (\rho_{Ni} \ell_i r_i f_i)^2 \pi r_i^2 (2 - f_i)}{3r_i + 3.51r_i f_i + 4.51\ell_i}, \quad i = 1, 2.$$

The mutual inductance calculation is the integral for the cross section of each coil of the field along the center axis from a single loop multiplied by the area of a single receiving loop. Since this expression relies on Wheeler's approximation for the self inductance of a multi-layer coil, it shares the same limitations, namely, the aspect ratio (a.r.) of the coils, $\ell_i/(r_i f_i)$ must be close to 1, or $1/2 < \ell_i/(r_i f_i) < 2$. However, there are widely known approximations for other aspect ratios that would result in similar expressions [5].

The resulting expression for the magnetic coupling coefficient κ is

$$\begin{aligned} \kappa = \frac{L_M}{\sqrt{L_1 L_2}} = & \frac{\sqrt{3r_1 + 3.51r_1 f_1 + 4.51\ell_1} \sqrt{3r_2 + 3.51r_2 f_2 + 4.51\ell_2} r_1 r_2}{2 - f_1 \quad 2 - f_2 \quad 4f_1} \left(\frac{f_2^2}{3} - f_2 + 1 \right) \times \dots \\ & \sum_{i=1..4} (-1)^i \left[\sqrt{1 + \left(\frac{s + \ell_i}{r_1} \right)^2} - (1 - f_1) \sqrt{(1 - f_1)^2 + \left(\frac{s + \ell_i}{r_1} \right)^2} + \dots \right. \\ & \left. \left(\frac{s + \ell_i}{r_1} \right)^2 \arcsin \frac{r_1}{s + \ell_i} - \left(\frac{s + \ell_i}{r_1} \right)^2 \arcsin \frac{r_1(1 - f_1)}{s + \ell_i} \right], \quad \ell_i = \{0, \ell_1, \ell_1 + \ell_2, \ell_2\}. \end{aligned}$$

The first term of the Taylor series expansion of this expression provides an upper bound, κ_u , for the magnetic coupling coefficient as the separation s tends to infinity, where

$$\begin{aligned} \kappa_u = & \frac{1}{2} r_1 \sqrt{3r_1 + 3.51r_1 f_1 + 4.51\ell_1} \left(\frac{f_1^2/3 - f_1 + 1}{2 - f_1} \right) \times \dots \\ & r_2 \sqrt{3r_2 + 3.51r_2 f_2 + 4.51\ell_2} \left(\frac{f_2^2/3 - f_2 + 1}{2 - f_2} \right) \frac{1}{s^3}, \end{aligned}$$

as shown in Figure 2. Adding the second term of the Taylor series expansion results in a lower bound for the magnetic coupling coefficient, κ_l , where

$$\kappa_l = \kappa_u \left(1 - \frac{3}{2} \frac{\ell_1 + \ell_2}{s} \right),$$

also shown in Figure 2. Even though the value of the magnetic coupling coefficient in this range is on the order of 10^{-2} to 10^{-4} , large enough quality factors in resonant systems may allow the transfer of power at high enough magnitude and efficiency for some applications [11].

The upper and lower bounds for the coupling coefficient also let us determine when the upper bound approximation for κ is an appropriate substitute. The normalized difference between the bounds is

$$\frac{\kappa_u - \kappa_l}{\kappa_u} = \frac{3}{2} \frac{\ell_1 + \ell_2}{s}.$$

This expression can be solved for s to indicate the range of separations where the magnetic coupling coefficient is arbitrarily close to its limit κ_u .

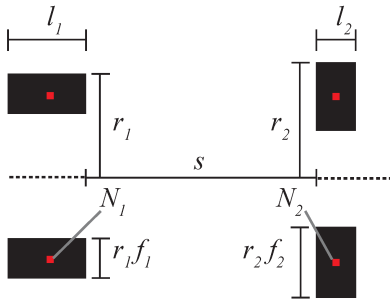


Figure 1. Cross-section diagram of the coil geometry. Sender and receiver coils are multilayer, axially aligned with length l_i , outer radius r_i , turns N_i , and thickness $r_i f_i$, where $0 < f_i < 1$ is the fill. The separation between coils is s . The turns density ρ_{N_i} is defined as $N_i / (l_i r_i f_i)$.

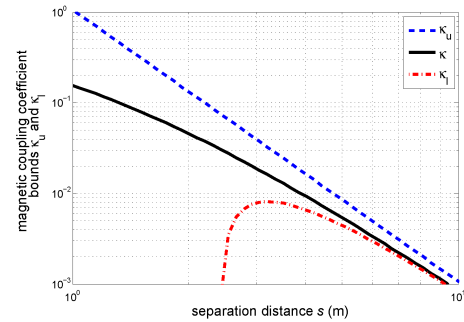


Figure 2. Long-range approximation for the magnetic coupling coefficient κ and bounds κ_u and κ_l as a function of separation distance s for identical sender and receiver coils of radii $r_i = 1$ m, aspect ratio 2, and fill $f = 0.4$. As expected, both the approximation for κ and κ_l converge to κ_u as s approaches infinity.

3. Normalization

The upper bound for the magnetic coupling coefficient, κ_u , suggests a normalized separation distance δ , where

$$\delta = s / \sqrt{(V_{\text{eff},1})^{1/3} \cdot (V_{\text{eff},2})^{1/3}}$$

and

$$V_{\text{eff},i} = \left[3 + 3.51 f_i + 4.51 l_i / r_i \right] \left[\frac{f_i^2 / 3 - f_i + 1}{2 - f_i} \right]^2 r_i^3, \quad i = 1, 2.$$

Since the quantity V_{eff} has units of volume, we call it the *effective magnetic volume*. As shown in Figure 3, this normalization simplifies the limit behavior of any pair of coils to

$$\kappa_u = 1 / 2 \delta^3.$$

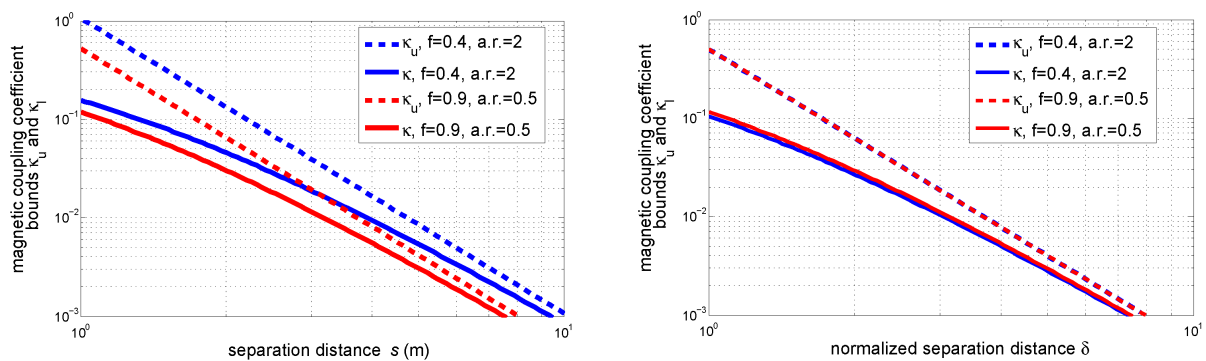


Figure 3. Long-range approximation for the magnetic coupling coefficient κ and upper bound κ_u as a function of separation distance s and normalized separation distance δ for two sets of identical sender and receiver coils. The first set has radii $r_i = 1$ m, aspect ratio 2, and fill $f = 0.4$. The second set has radii $r_i = 1$ m, aspect ratio 1/2, and fill $f = 0.9$. As expected, the limit κ_u is identical for both sets when plotted against the normalized separation distance δ .

4. Validation

The expressions derived for the magnetic coupling coefficient and its bounds were validated experimentally by measuring the voltage induced by a sender coil on an axially aligned receiver coil as shown in Figure 4. The experiment was repeated using three different coil pairs. The circuit model of the experimental system ignores the load presented by the measuring probes and assumes no current in the receiver coil. The sender coil was driven with a sinusoidal voltage v_S of 1.64 Vrms. The frequency was adjusted until the phase difference between the voltages across the sender v_S and receiver v_2 was 45 degrees, such that

$$\left| \frac{v_2}{v_S} \right| = \frac{\kappa}{\sqrt{2}} \sqrt{\frac{L_2}{L_1}},$$

where v_2 is the voltage across the receiver coil, L_2 is the inductance of the receiver coil, L_1 is the inductance of the sender coil, and v_S is the voltage across the sender coil.

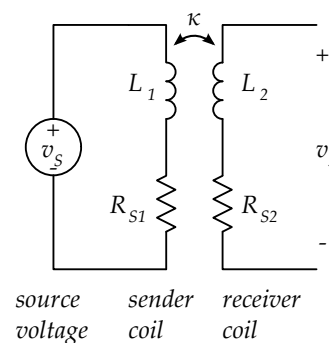
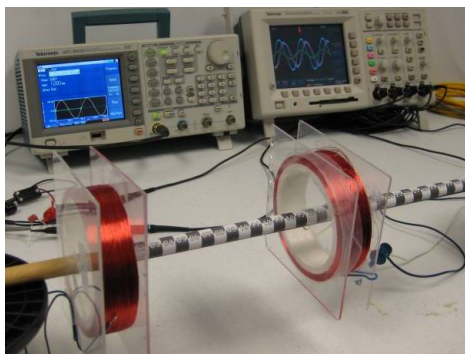


Figure 4. Experimental system for measuring the magnetic coupling coefficient between two axially aligned coils and circuit model. A sender coil of inductance L_1 is driven using a voltage source v_S . The induced voltage v_2 is measured across an axially aligned receiver coil of inductance L_2 . The source coil is driven at the frequency $R_{S1}/(2\pi L_1)$ such that the measurement is independent of R_{S1} .

In two experiments, shown in red and blue in Figure 5, the sender coil had an outer radius $r_1 = 5$ cm, inner radius of 4.5 cm (for a resulting fill factor $f_1 = 0.1$), length $\ell_1 = 2.5$ cm and a measured inductance of $L_1 = 0.74$ H. The first experiment, shown in red in Figure 5, had a receiving coil with dimensions and inductance identical to the transmitting coil. The second experiment, shown in blue in Figure 5, had a receiver coil with an outer radius $r_2 = 7$ cm, inner radius of 6.5 cm (for a resulting fill factor $f_2 = 0.07$), length $\ell_2 = 2.5$ cm and a measured inductance of $L_2 = 2.76$ H.

In the third experiment, shown in purple in Figure 5, the sender coil was the receiver coil from the second experiment with a measured inductance of $L_1 = 2.76$ H. The receiver coil had an outer radius $r_2 = 6.5$ cm, inner radius of 4.5 cm (for a resulting fill factor $f_2 = 0.31$), length $\ell_2 = 8.9$ cm and a measured inductance of $L_2 = 2.5$ H.

5. Conclusion

The universal behavior resulting from the normalized separation δ can be used to maintain the same limit behavior of the magnetic coupling coefficient while changing the dimensions of either coil. In particular, the limit behavior will be the same as long as the geometric mean of effective magnetic volumes of the coils remains constant. Alternatively, the effective magnetic volume can be used to maximize the limit behavior of the magnetic coupling coefficient by optimizing the geometry of coils given any set of constraints.

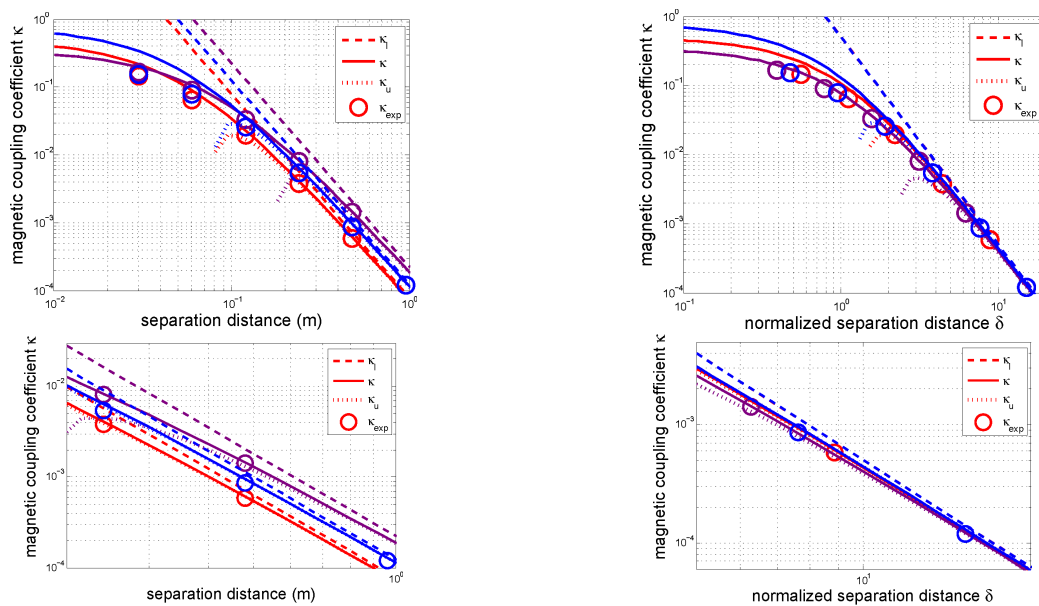


Figure 5. Magnetic coupling coefficient κ as a function of separation s and normalized separation δ for three different coil pairs. The solid lines are the long-range approximation for the magnetic coupling coefficient κ , the dashed lines are the upper bounds κ_u , the dotted lines are the lower bounds κ_l , and the circles are empirical results derived from measurements of the voltage induced in the receiver coil. The bottom graphs shown the largest measured separation to show the convergence when the separation distance is normalized.

Acknowledgements

The authors wish to acknowledge the help of Evan Dorksy in the data collection and analysis for the experimental portion of the paper.

References

- [1] L. Rindorf, L. Lading and O. Breinbjerg, "Resonantly coupled antennas for passive sensors," *IEEE Sensors Conferences*, pp. 1611-1614, 2008
- [2] A. Kumar, S. Mirabbasi and M. Chiao, "Resonance-based Wireless Power Delivery for Implantable Devices," pp. 25-28, 2009.
- [3] J. C. Maxwell and J. J. Thompson, "Potential of two parallel circles expressed by elliptic integrals," in *A treatise on electricity and magnetism*, Oxford, 1873, pp. 338-350.
- [4] E. B. Rosa, "The Self and Mutual Inductances of Linear Conductors," *Bulletin of the Bureau of Standards*, vol. 4, no. 2, pp. 302-344, 1908.
- [5] H. A. Wheeler, "Simple Inductance Formulas for Radio Coils," vol. 16, no. 10, pp. 1398-1400, 1928.
- [6] A. P. Sample, M. A. David and J. R. Smith, "Analysis, Experimental Results, and Range Adaptation of Magnetically Coupled Resonators for Wireless Power Transfer," *IEEE Transactions on Industrial Electronics*, vol. 58, no. 2, pp. 544-554, 2001.
- [7] J. T. Conway, "Exact Solutions for the Magnetic Fields of Axisymmetric Solenoids and Current Distributions," *IEEE Transactions On Magnetics*, vol. 37, no. 4, pp. 2977-2988, 2001
- [8] H. Nagaoka, "The Inductance Coefficients of Solenoids," *Journal Of the College of Science, Imperial University*, vol. 27, no. 6, pp. 1-33, 1909.
- [9] S. Hui, C. K. Lee and W. X. Zhong, "Recent Progress in Mid-Range Wireless Power Transfer," pp. 3819-3824, 2012.
- [10] J. O. Mur-Miranda, G. Fanti, Y. Feng, K. Omanakuttan, R. Ongie, A. Setjoadi, and N. Sharpe, "Wireless power transfer using weakly coupled magnetostatic resonators," in *IEEE Energy Conversion Congress and Expo (ECCE 2010)*, September 12-16, 2010.
- [11] J. O. Mur-Miranda, and G. Fanti, "Peak wireless power transfer using magnetically coupled series resonators," in *IEEE Energy Conference and Exhibition (EnergyCon 2010)*, December 18-22, 2010.